# Test with cosmic rays of the GEM chambers for the LHCb muon system produced in Cagliari

## Public Note

Issue: 1
Revision: 0

Reference: CERN-LHCb-2007-132-MUON
Created: October 26, 2007
Last modified: October 26, 2007

**Prepared by:**
W. Bonivento[a], A. Cardini[a], R.G.C. Oldeman[a], D. Raspino[a], B. Saitta[a]

[a]Università and INFN, sezione di Cagliari

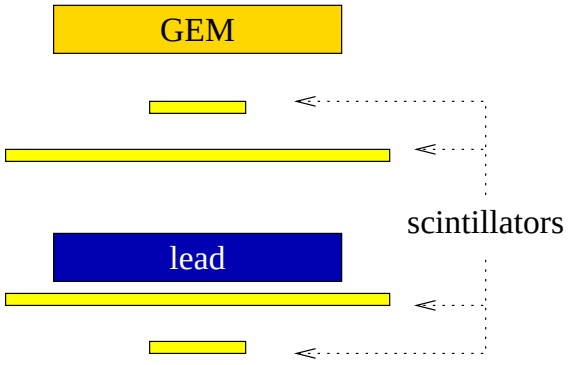


**Figure 1** Sketch of the experimental setup.

## Abstract

The inner region of the first LHCb muon station will be equipped with twelve Gas Electron Multiplier chambers. The seven chambers produced in Cagliari were studied for several days each using cosmic rays. We measured the efficiency, timing resolution, and uniformity, cluster-size and out-of-time multiplicity. We find all seven chambers perform well.

## 1 Introduction

The LHCb muon system consists of 5 stations, called M1–M5, each divided into 4 regions, R1–R4 with a granularity depending on the distance from the beam pipe [1]. Being positioned in front of the calorimeter, the first muon station (M1) of LHCb is exposed to all particles originating directly or indirectly from the primary $pp$ collision. This results in an equivalent particle rate of up to $1.4 \times 10^5\,\mathrm{s}^{-1}\mathrm{cm}^{-2}$ in the inner region [2]. To cope with these high rates, a solution based on three-stage Gas Election Multipliers (GEM) with an $\mathrm{Ar}/\mathrm{CO}_2/\mathrm{CF}_4$ gas mixture was chosen.

Twelve GEM chambers surround the beam-pipe. Each chamber consists of two gaps with 192 pads of 1.0 cm by 2.5 cm, organized as 8 rows of 24 pads. Every chamber has 24 front-end boards (CARDIAC-GEM), containing two CARIOCA-GEM chips [3] that amplify, discriminate, and shape the signals from 8 pads on each gap, and one DIALOG [4] chip that adjusts the timings and produces the logical OR of the signals from the two gaps.

Once completely assembled we test the chambers with cosmic rays. This allows us to verify the functionality of the chambers and to study and compare their properties.

## 2 Description of the cosmic ray setup

We use two large scintillators with an active area of 30 cm by 30 cm to provide an external trigger on the occurrence of a cosmic ray. The two large scintillators are separated vertically by 25 cm. In between the scintillators, 5 cm of lead selects cosmic rays with a momentum of at least 70 MeV/$c$. The rate of the trigger, corresponding to the AND of the two large scintillators, is approximately 4 Hz.

In addition, the signals from two smaller scintillators, with an active area of 10 cm by 10 cm, are included in the data stream to select cosmic rays of mostly vertical incidence over a well-defined area of the GEM chamber. They are separated vertically by 30 cm, thus the maximum angle with the vertical is 25°. A sketch of the layout is shown in Figure 1.

While early tests were done with the chamber in between the two scintillators, all measurements reported here are performed with the chamber positioned above all scintillators. This allowed for quicker mounting and dismounting of the chambers. In addition, the larger area of the GEM chamber

| Nominal gain | 1000 | 2000 | 3000 | 4000 |
|---|---|---|---|---|
| GEM1 down | 500.0 | 500.0 | 500.0 | 500.0 |
| GEM1 up | 891.9 | 903.8 | 910.8 | 915.7 |
| GEM2 down | 1592.0 | 1604.0 | 1611.0 | 1615.5 |
| GEM2 up | 1984.0 | 2007.5 | 2021.5 | 2031.5 |
| GEM3 down | 2334.0 | 2357.5 | 2371.5 | 2381.5 |
| GEM3 up | 2754.0 | 2790.5 | 2811.5 | 2827.0 |
| Cathode | 3804.0 | 3840.5 | 3862.0 | 3877.0 |

**Table 1** High voltage settings (in Volts) on the GEMs.

within the acceptance of the small scintillators results in a more homogeneous illumination of the chamber for the efficiency measurement.

Every tested chamber is fully equipped with the 24 calibrated CARDIAC-GEM boards. The LVDS (Low Voltage Differential Signal) outputs, which on LHCb will be readout by the ODE (On Detector Electronics) boards, are instead converted into ECL signals and readout using 3 VME TDCs (two 64 channel V767A and one 128 channel V767) with 0.8 ns bins. Low voltage for the 24 CARDIAC-GEM boards is supplied by 3 HAMEG 7042-4 low-voltage (LV) supplies, regulated by a custom-made GEM-LV regulator. Each gap requires 7 independent negative high voltage (HV) channels, two for each side of each GEM foil plus one for the cathode; the pads serve as anode and are coupled to the CARIOCA-GEM input, at $\approx 0$ V.

After construction, the chambers are continuously flushed with nitrogen gas. After mounting on the test setup, the chambers are flushed for at least 12 hours with the nominal gas mixture (Ar:$CO_2$:$CF_4$ 45:15:40) and a flux of 100 $cm^3$/min. Since each gap has a gas-volume of about 700 $cm^3$ and the gas passes through both gaps in series, the gas is refreshed at least 100 times before the HV is switched on.

The communication with the DIALOG chips on each CARDIAC-GEM board occurs through an $I^2C$ interface, using four $I^2C$ chains that serve six CARDIAC-GEM boards each. The threshold of the CARIOCA-GEM has been set to 2.8 fC for all CARDIAC-GEM boards for all chambers. The HV settings for the nominal electron multiplication gain are summarized in Table 1.

# 3 Results

The data taking program for each chamber was limited by the available time, approximately five weeks, between completion of the chambers and shipment to CERN in July 2007.

The baseline data taking program for each chamber comprises:

- 200,000 triggers ($\approx 14$ h) with gap A at a nominal gain of 4000 and the gap B off, and 200,000 triggers with gain(B)=4000, gain(A)=0. This allows to study each gap with high statistics at their nominal working point.
- 50,000 triggers ($\approx 3.5$ h) with gain(A)=2000, gain(B)=0, and 50,000 triggers with gain(B)=2000, gain(A)=0. Idem for a gain of 1000. This allows to study the turn-on of the efficiency for both gaps.
- 50,000 triggers ($\approx 3.5$ h) with gain(A)=4000, gain(B)=4000, readout of the OR-ed signals. This corresponds to the actual operating condition at LHCb.

Due to time constraints, for some chambers the baseline program could not be fully completed, while for other chambers, the baseline program could be extended with either extended data taking or additional configurations.

The centering of the timing window has been determined for each run by finding the 20 or 50 ns window with the largest number of hits.

## 3.1 Channel multiplicity

Figures 2 and 3 show the hit multiplicity of the gaps at a nominal gain of 4000, accepting all triggers. We see five dead channels on a total of 2688. The two dead channels of gap A, chamber G and the one dead channel of gap A, chamber C are related to faulty CARDIAC-GEM cards that have been replaced in the meanwhile. There was no time to redo the full measurement after replacement of the cards, but we verified with shorter runs that the channels detect hits. The two dead channels of gap A, chamber E instead were due to missing connections between the chamber and the signal connector. They have been fixed after arrival at CERN.

## 3.2 Average pulse arrival time

Figures 4 and 5 show the average arrival time of pulses at a nominal gain of 4000, accepting all triggers. A window of 50 ns has been applied to reduce the influence of out-of-time hits. Significant non-uniformities at the level of 12 ns can be seen. Part of this is due to the response of the cosmic ray setup, and is seen in all gaps. However, some chambers, in particular gap B, chamber B have an additional structure in the average arrival time. If left uncorrected, this results in a deteriorated timing performance of the chamber as a whole. However, it is possible at the level of the DIALOG chip to perform a fine timing correction, where the delay in every channel can be adjusted in steps of 1.6 ns. This data indicates that to achieve the best timing resolution, such a calibration will need to be done.

Since the cosmic ray setup is affected by spatially correlated timing differences due to the use of scintillator triggers readout on one side, we do not plan to use the cosmic ray data for fine timing calibration. Instead we anticipate to perform this fine timing using the first collision data.

## 3.3 Pulse arrival time distribution

Figures 6 and 7 show the average arrival time of pulses at a nominal gain of 4000, accepting only triggers that pass through the small scintillators. Beside the main peak, corresponding to in-time hits, we see a second peak at later times. While this effect has not been completely understood, individual inspection of events indicate that these come from a few events with a very high hit multiplicity. Most likely, these originate from the currents associated with the charge redistribution of the whole chamber following a particularly strong electron cascade from a heavily ionizing particle, for example a low-momentum nuclear fragment.

## 3.4 Efficiency

Figures 8 and 9 show the efficiency of the GEMs at different gains in a 20 ns and a 50 ns window respectively. The 20 ns window corresponds to the nominal running at LHCb, for a 25 ns bunch crossing, and allowing for up to 5 ns of timing misalignment. Most of the inefficiency in the 20 ns time window is not from missing hits, but due to hits being registered either too early or too late. Therefore we also quote the efficiency in a 50ns time-window, which corresponds to the efficiency of producing any hit.

The efficiency is measured as the fraction of events that produce one or more GEM hit in the time window, compared to all cosmic rays that fire both the large and the small scintillators. This cannot be interpreted as the absolute efficiency: At earlier measurements with cosmic rays at higher gains, the efficiency measured this way would never surpass 98.5%, while test-beam measurements showed an efficiency reaching 100.0% at high gain [5]. We hypothesize that a small fraction of the cosmic rays that we trigger on actually consist of two or more cosmic rays that fire the scintillators but do not traverse the GEM chambers.

Since a measurement of the absolute efficiency was not an aim of this study, we did not invest further effort in improving the experimental setup to identify a sample of ultra-pure cosmic rays needed for the determination of the absolute efficiency.

### 3.5 Peak time position and width

We make a Gaussian fit to the central 20 ns of the pulse arrival time, for cosmic rays that satisfy both the small and the large scintillator requirement. Figure 10 shows the position of the peaks and Figure 11 shows the width of the peaks. We find a strong dependence of the timing peak position and the gain: going from a gain of 1000 to a gain of 2000 or from a gain of 2000 to a gain of 4000, the pulses arrive on average 4 ns earlier. The width of the pulse arrival time distribution also improves at higher gain: typically 8 ns at G=1000, 6.5 ns at G=2000 and 5.5 ns at G=4000. Note that this width includes both the time jitter of the cosmic ray setup and the disuniformities of the chamber.

### 3.6 Cluster size

Figures 12 and 13 show the cluster size of the GEMs at different gains in a 20 ns and a 50 ns window respectively. We measure the cluster size as the number of hits in a window of five pads around the first GEM hit of every event. For single-gap measurements, the cluster size is typically smaller than 1.05(1.10) in a 20(50) ns window. For the OR setting, the cluster size is significantly larger, around 1.3. This is related to the angular distribution of the cosmic rays, that can have an angle of up to 25° with respect to the vertical.

### 3.7 Out-of-time multiplicity

To quantify the effect of events with high hit multiplicity, discussed in Section 3.3, we measure the additional multiplicity due to these events. For each trigger that satisfies the large scintillator requirement, we count the number of hits in a $60 - 200$ ns time window after the beginning of the the 20 ns time window. The averages of these are shown in Figure 14. We find under all circumstances the additional occupancy from out-of-time hits to be less than 0.03 per physics hit.

## 4 Conclusions

We studied with cosmic rays the 7 LHCb muon chambers based on GEM technology produced in Cagliari. We measured the efficiency, timing resolution, and uniformity, cluster-size and out-of-time multiplicity. We find all seven chambers perform well. All five channels that appear dead in this study have in the meanwhile been repaired.

## 5 Acknowledgements

We thank Giovanni Passaleva for many suggestions for improvements of this note.

## 6 References

[1] "LHCb Muon System Technical Design Report" CERN-LHCC-2001-010, CERN-LHCC-2003-002, CERN-LHCC-2005-0012

[2] Martellotti, G; Santacesaria, R; Satta, A "Particle rates in the LHCb muon detector" CERN-LHCC-2001-010, CERN-LHCC-2003-002, CERN-LHCC-2005-0012

[3] W. Bonivento "Design and performance of the front-end electronics of the LHCb Muon Detector" Proceedings of the 11th Workshop on Electronics for LHC and Future Experiments, Heidelberg, Germany, 12 - 16 Sep 2005, pp.363-367 CERN-2005-011, CERN-LHCC-2005-038

[4] S. Cadeddu, V. De Leo, C. Deplano, A. Lai "DIALOG: an ASIC for timing of the LHCb muon detector" NIM A 518, (2004) 486-90.

[5] G. Bencivenni *et al.*, "Performance of a triple-GEM detector for high rate charged particle triggering," Nucl. Instrum. Meth. A **494** (2002) 156.

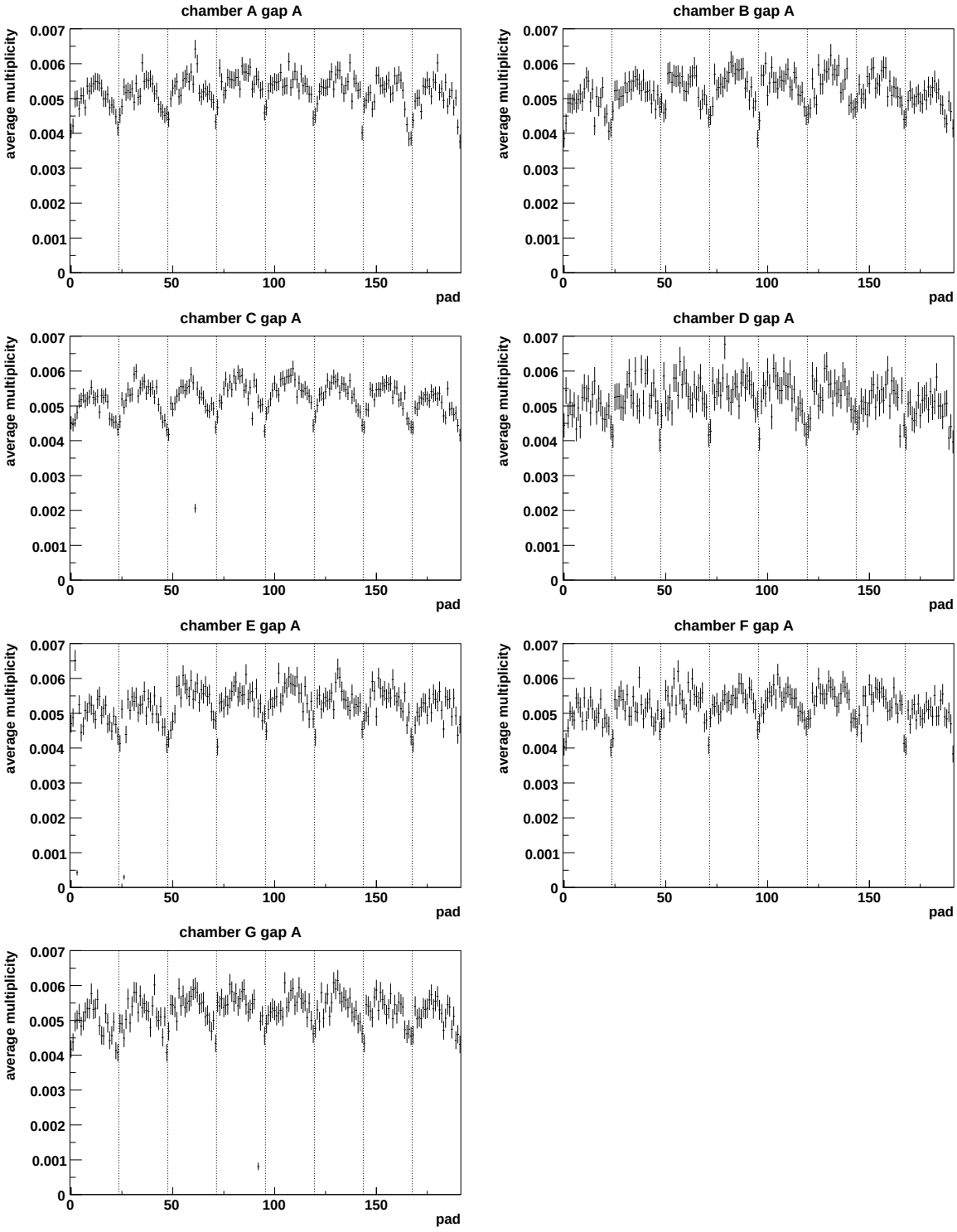


**Figure 2** Hit multiplicity of the A-gaps at a nominal gain of 4000.

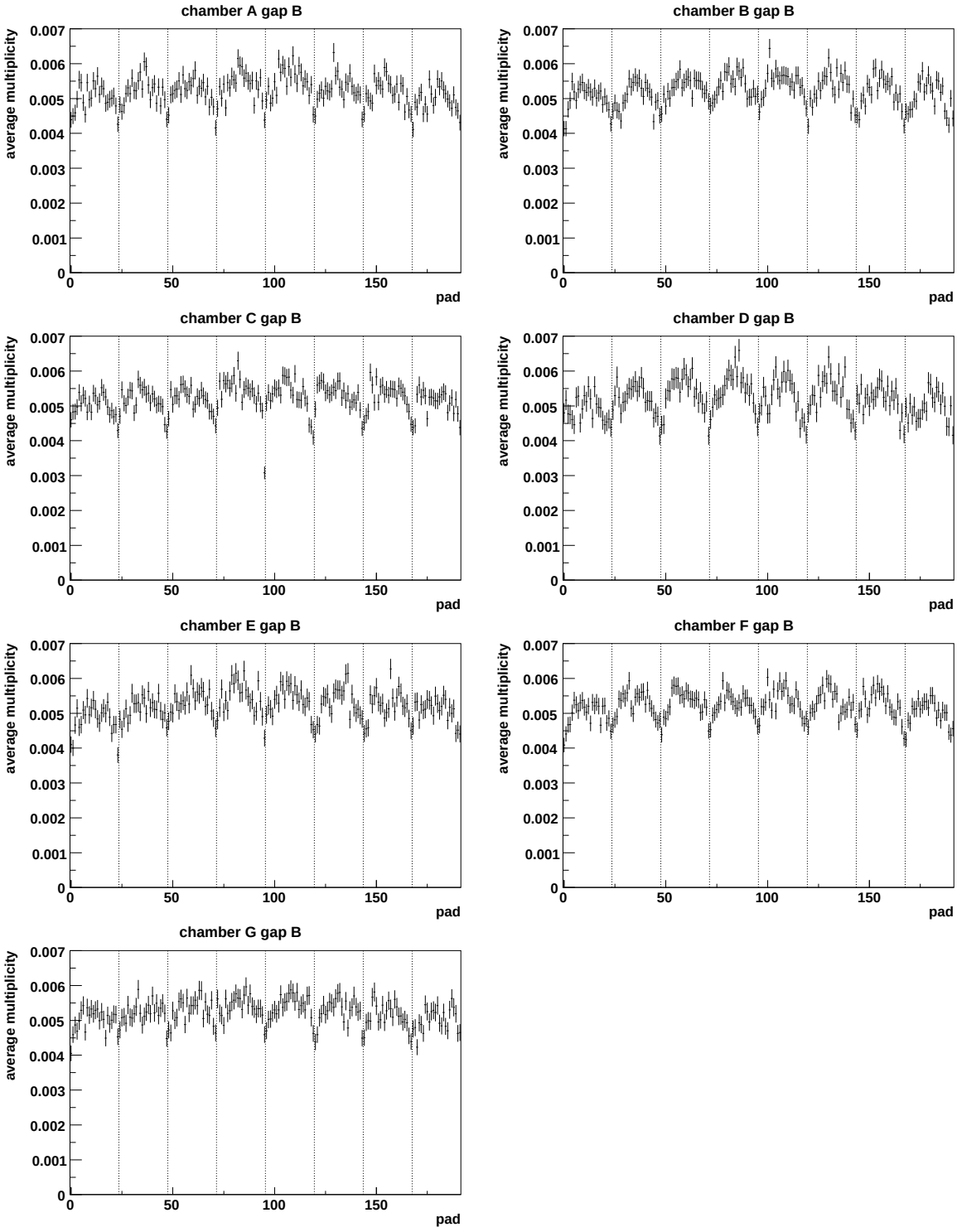


**Figure 3** Hit multiplicity of the B-gaps at a nominal gain of 4000.

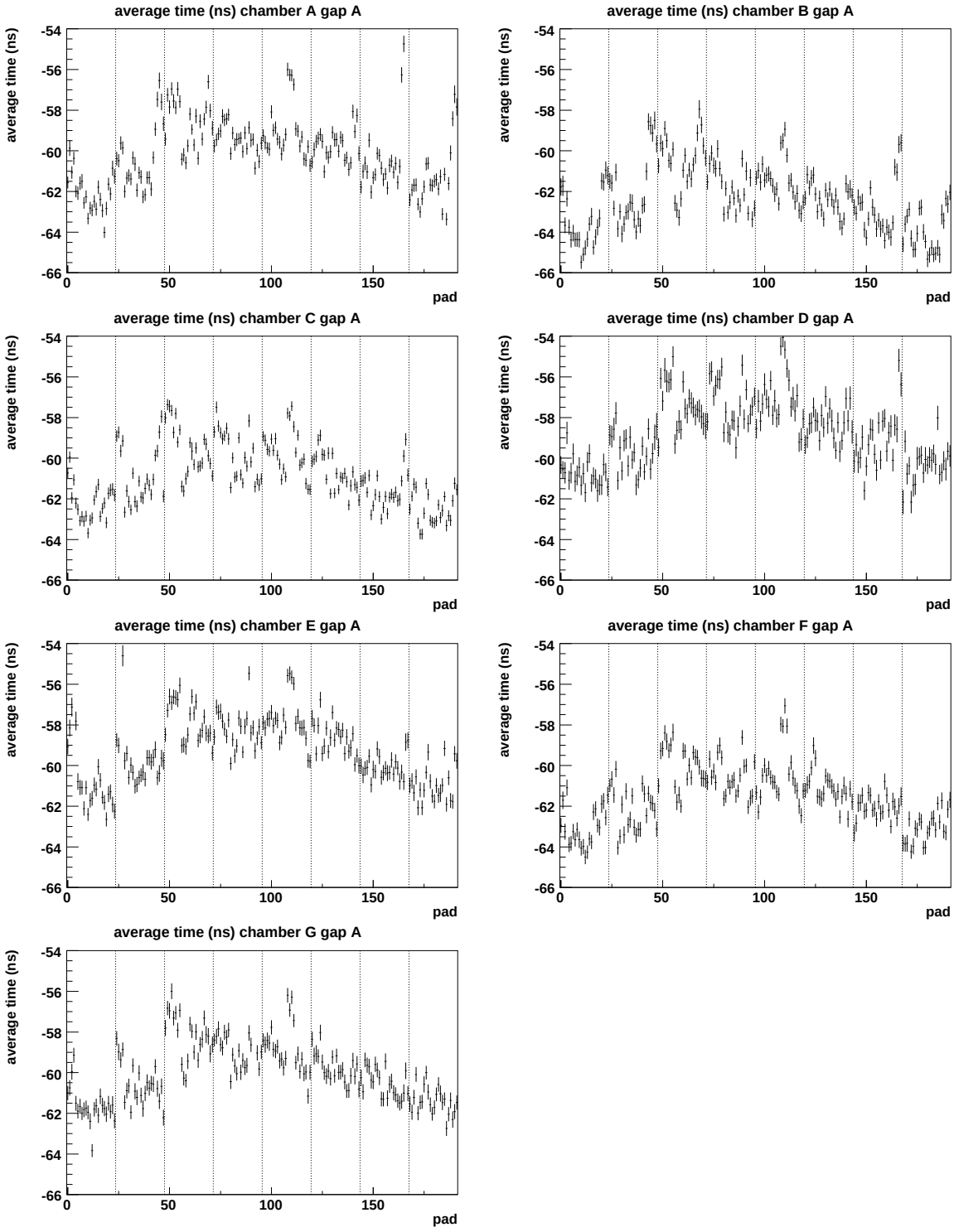


**Figure 4** Average pulse arrival time on the A-gaps at a nominal gain of 4000.

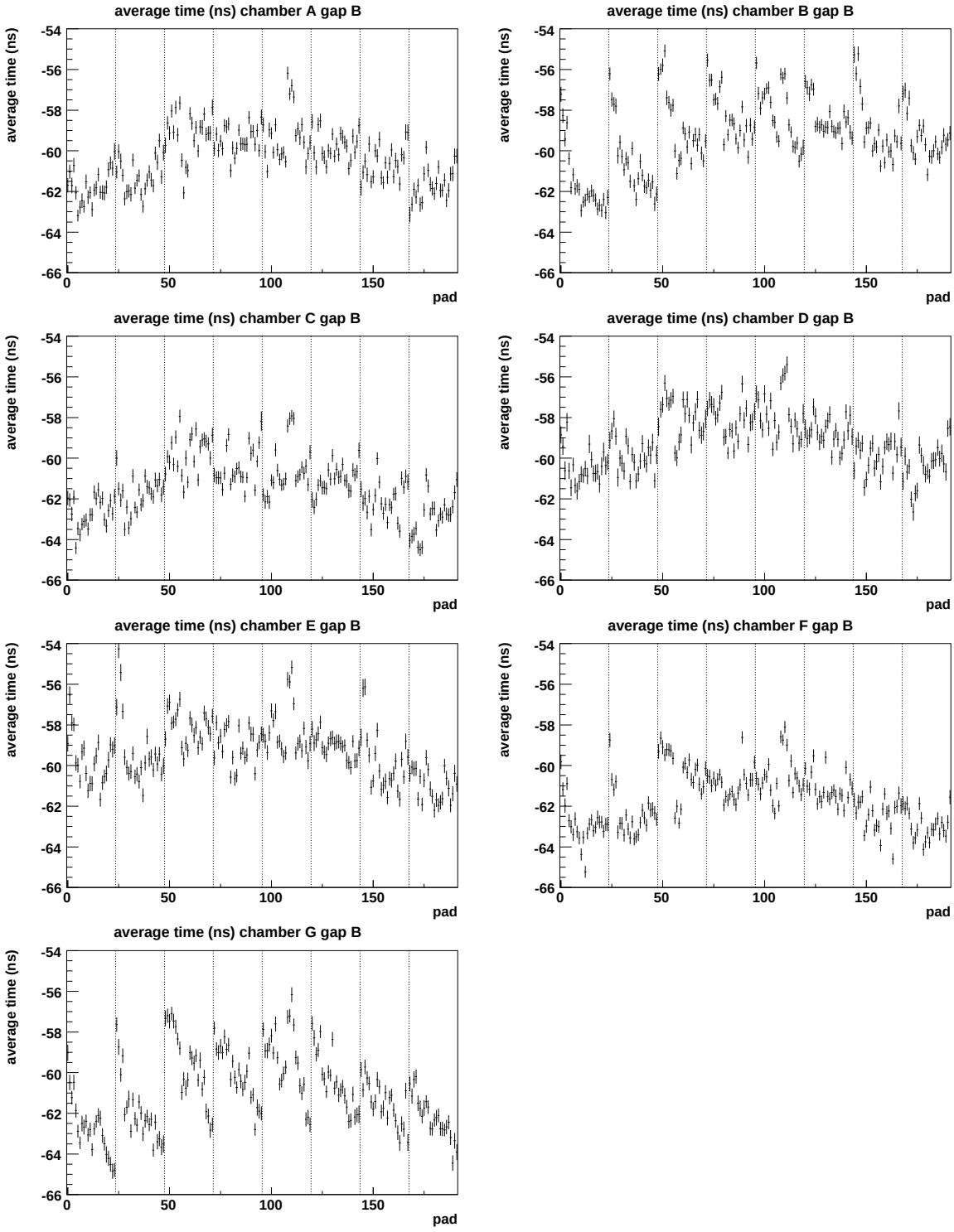


**Figure 5** Average pulse arrival time on the B-gaps at a nominal gain of 4000.

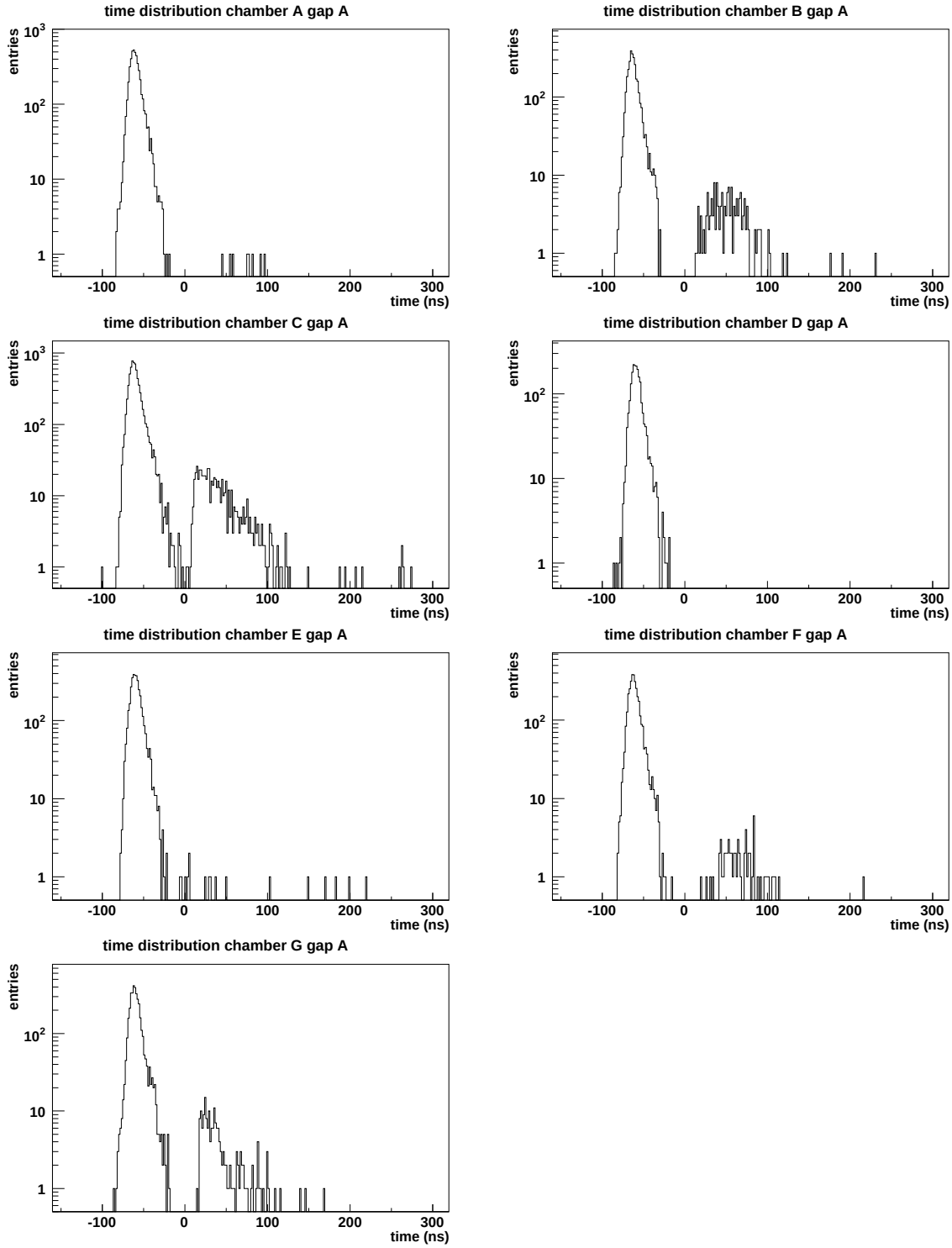


**Figure 6** Pulse arrival time distribution on the A-gaps at a nominal gain of 4000.

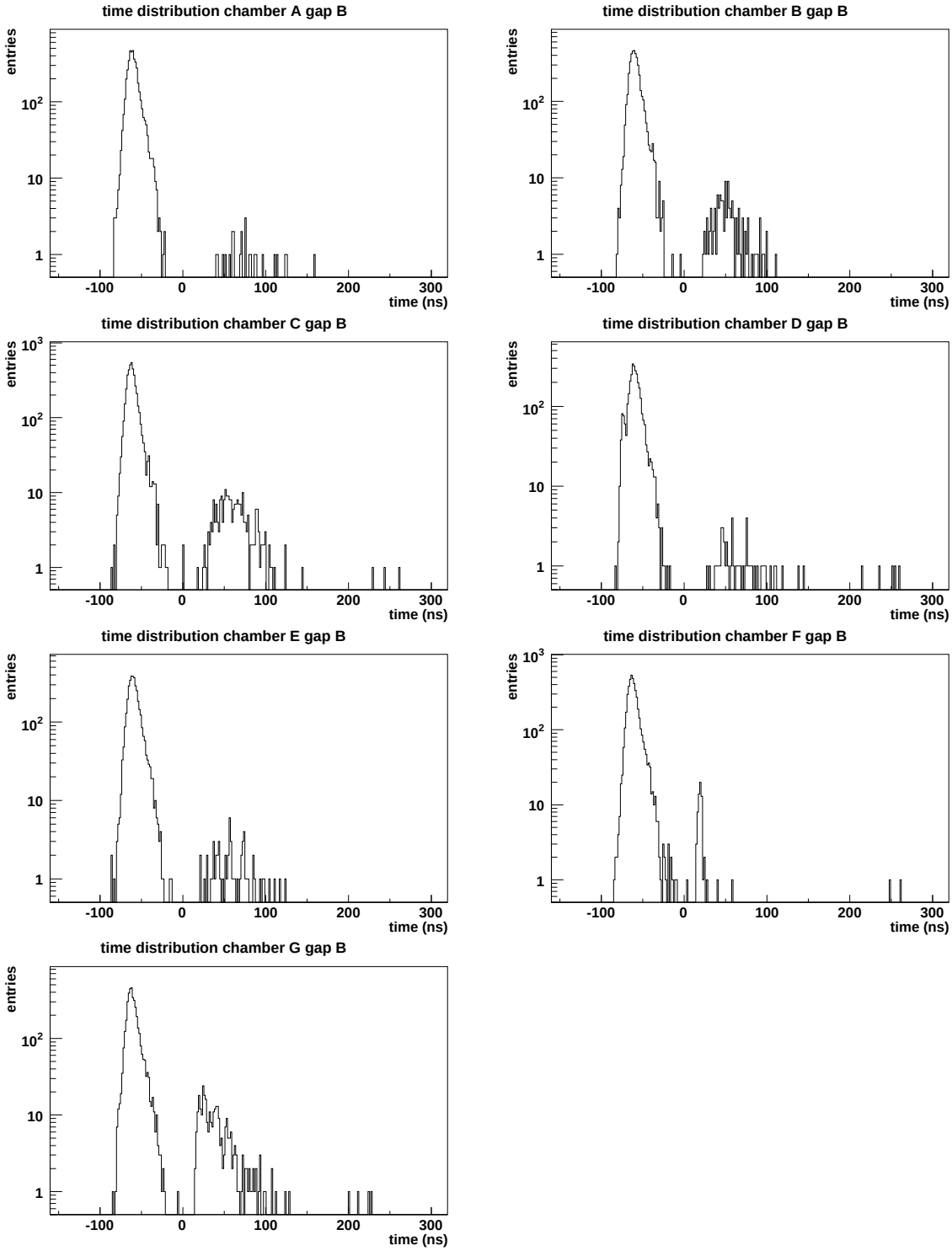


**Figure 7** Pulse arrival time distribution on the B-gaps at a nominal gain of 4000.

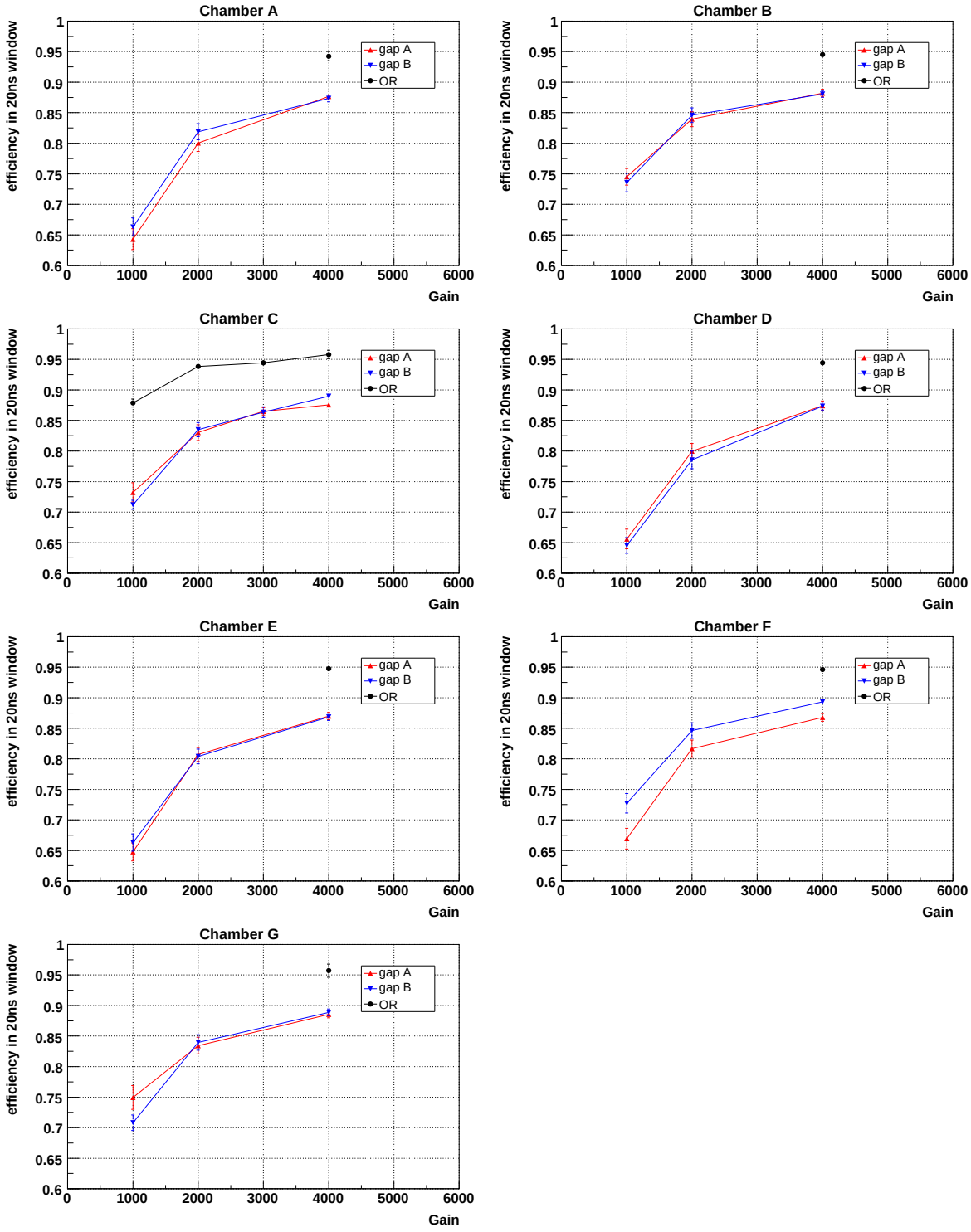


**Figure 8** Chamber efficiency for a 20 ns time window.

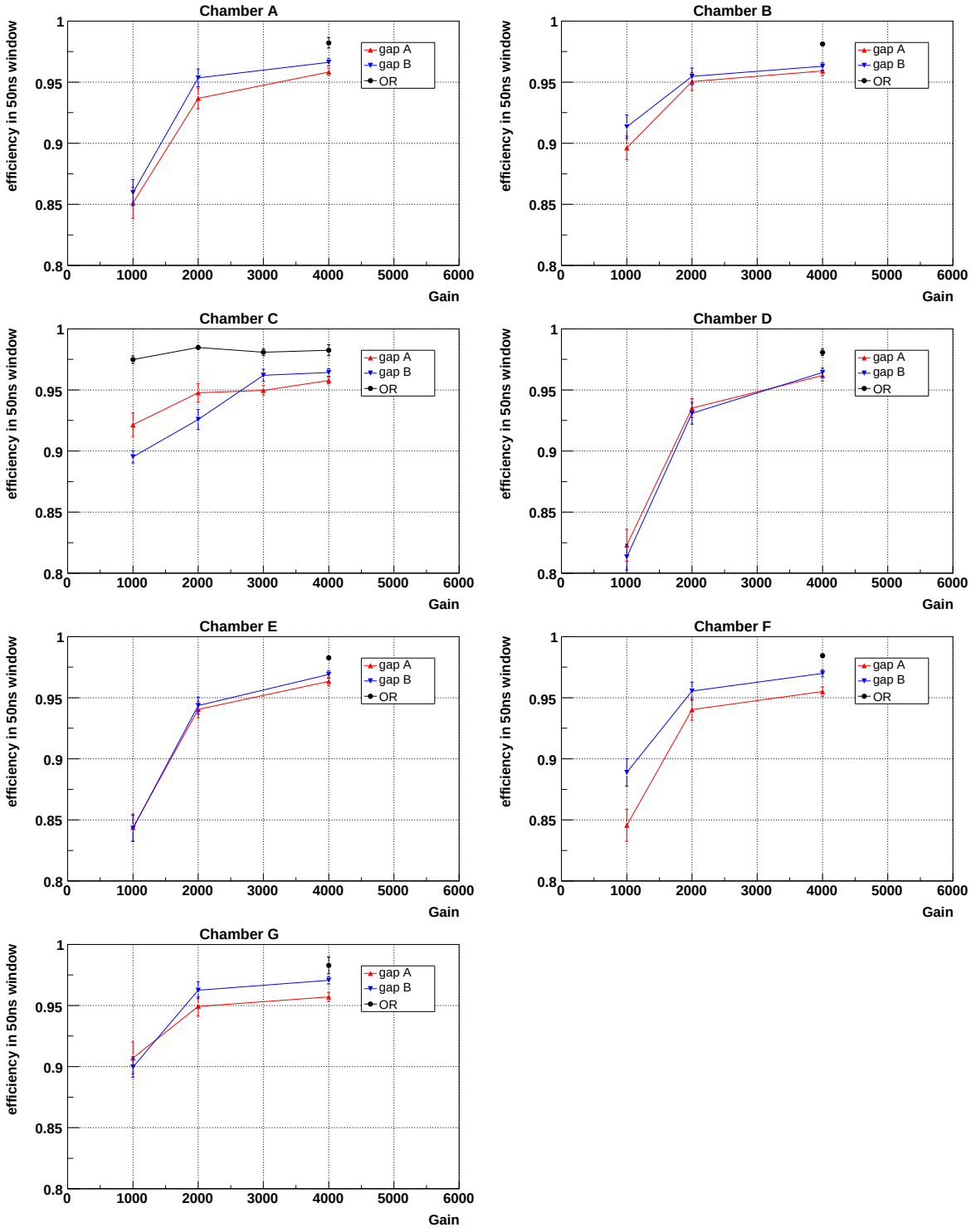


**Figure 9** Chamber efficiency for a 50 ns time window.

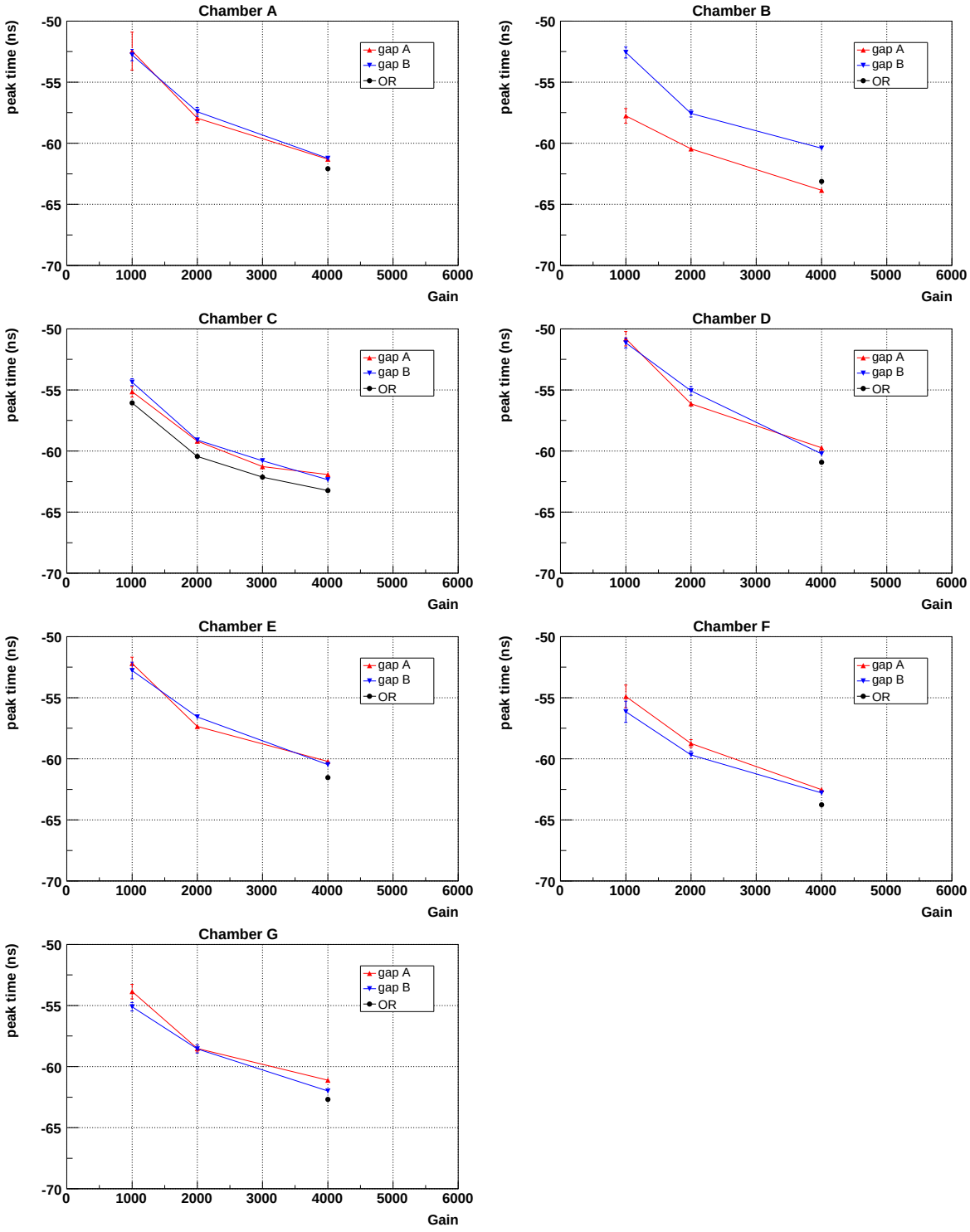


**Figure 10** Position of the peak of the pulse arrival time distribution.

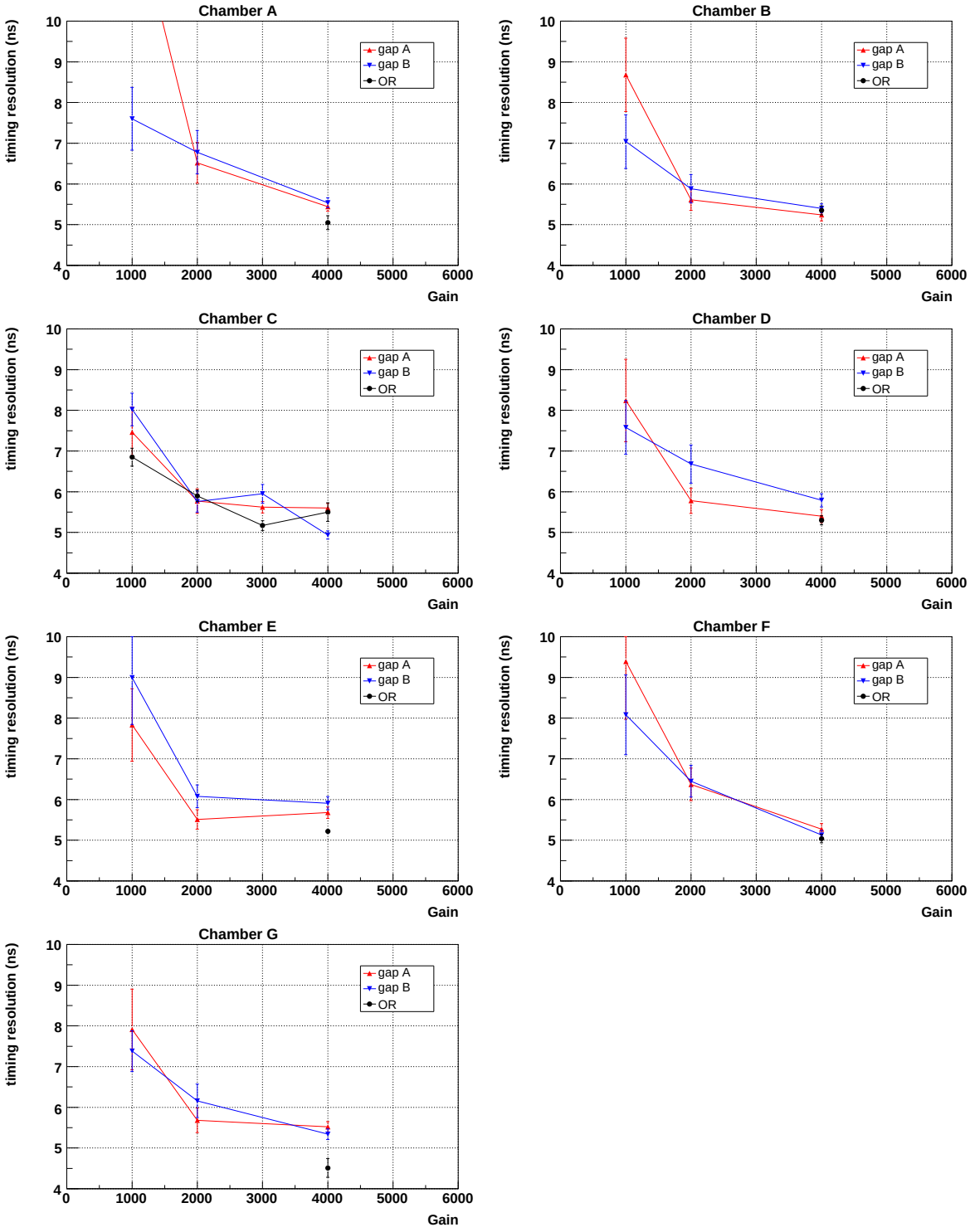


**Figure 11** Width of the peak of the pulse arrival time distribution.

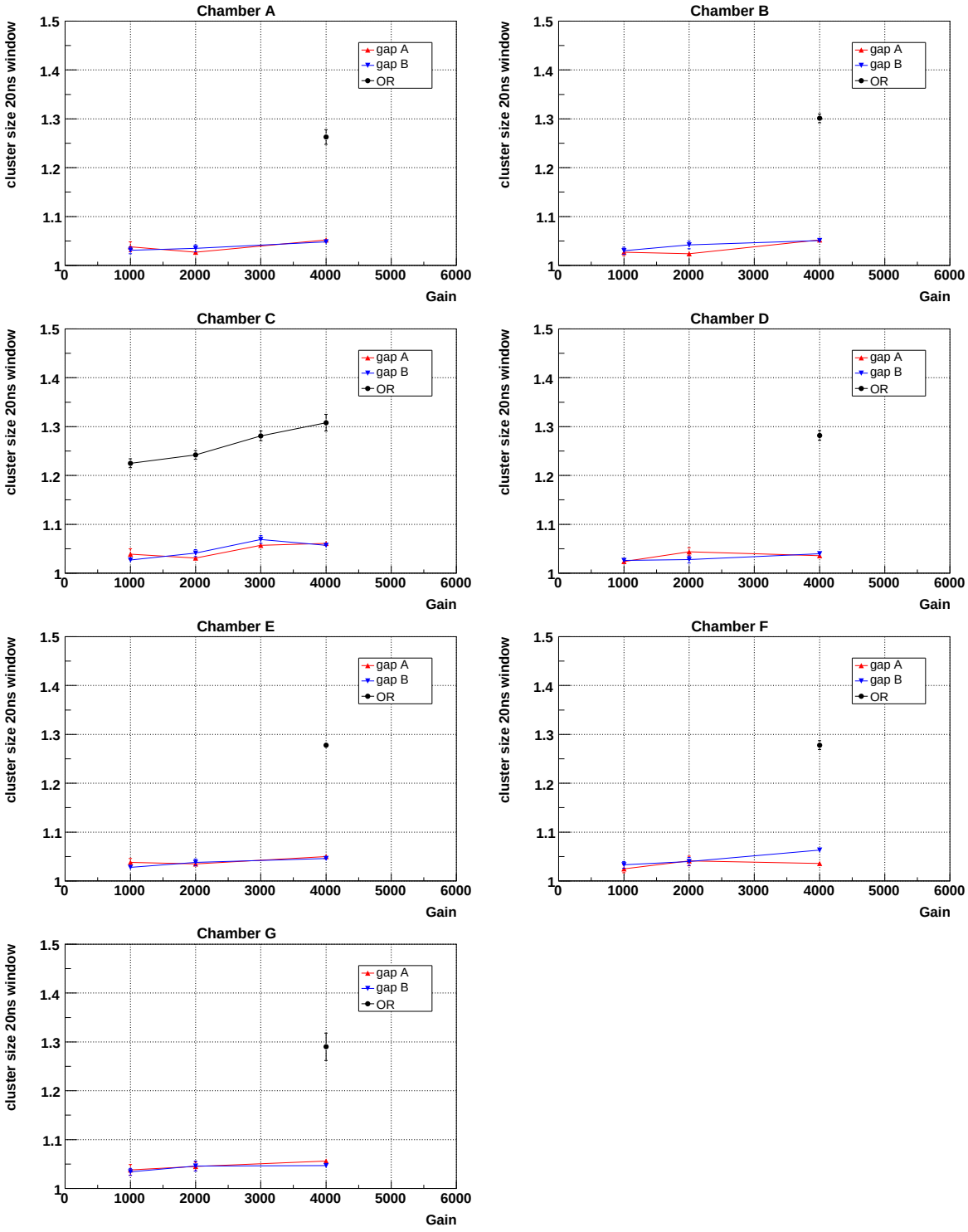


**Figure 12** Average cluster size for a 20 ns time window.

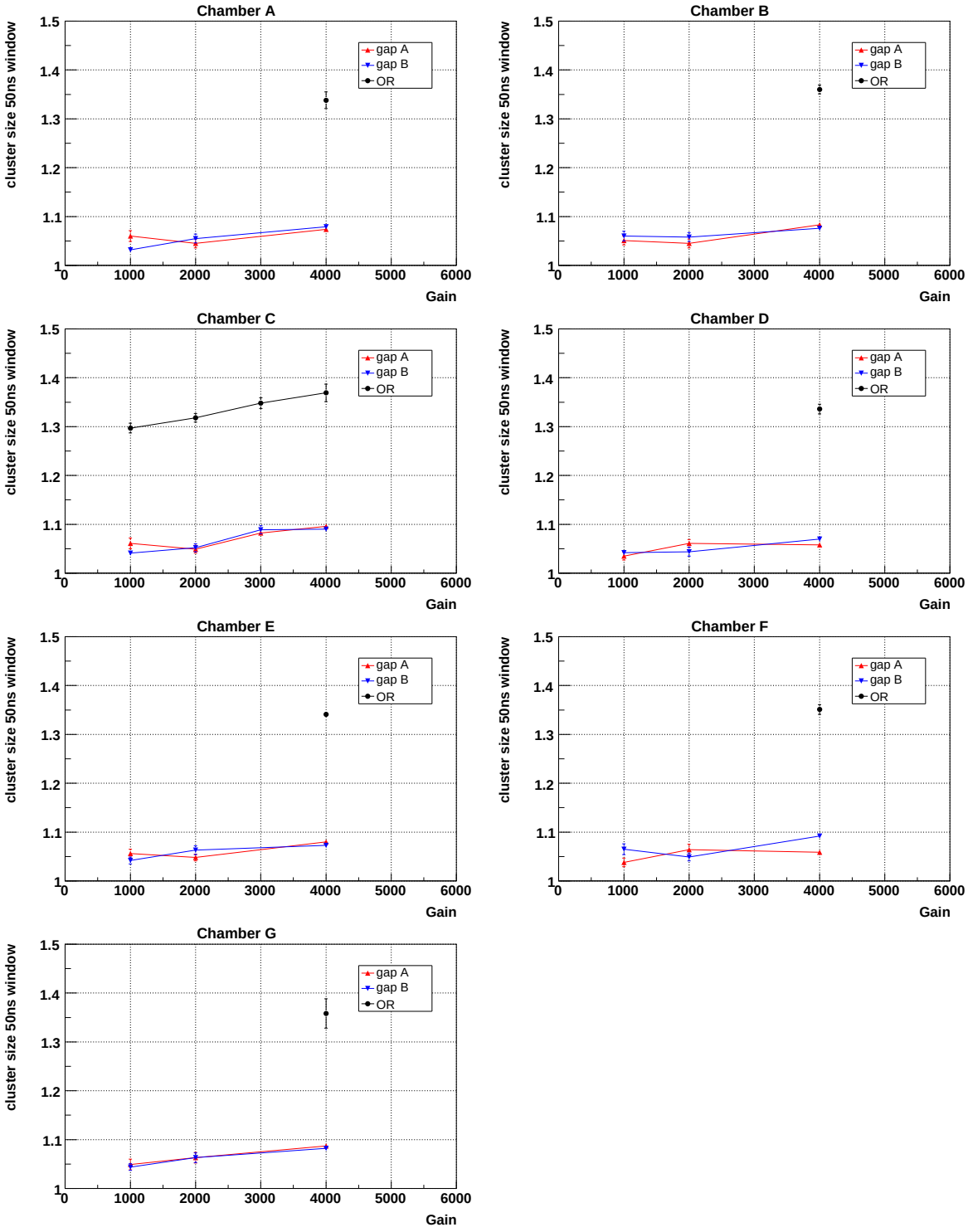


**Figure 13** Average cluster size for a 50 ns time window.

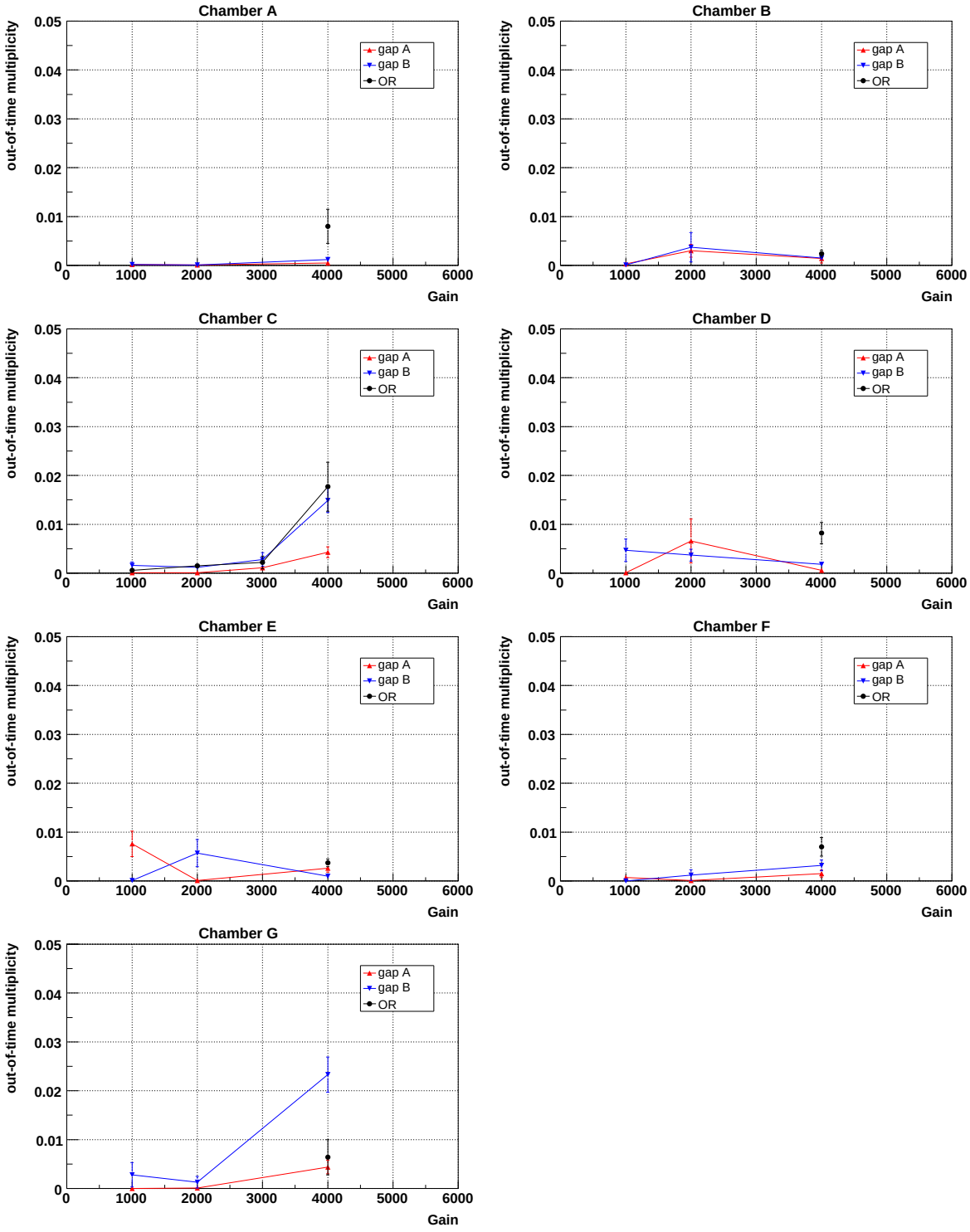


**Figure 14** Average out-of-time multiplicity.